A Vertical Conductor Circuit Model Including Up- and Down-ward Traveling Waves

A. Yamanaka, A. Hori, H. Murakami, N. Nagaoka

***Abstract*--A model of a vertical conductor for a circuit analysis is proposed based on calculation results by Finite-Difference Time-Domain (FDTD) method. The model expresses frequency-dependent effect of a vertical conductor. In addition, differences in its propagation characteristics of the upward and downward traveling waves are taken into consideration. An experiment is carried out using a reduced-size wind turbine tower model. The simulation results by Electromagnetic Transients Program (EMTP) accurately reproduce the experimental results.**

***Keywords*: vertical conductor, modeling, lightning, surge, traveling wave, FDTD method, EMTP.**

I. Introduction

MOST of the wind turbine power plants in Japan are constructed on top of hills or mountains to obtain good wind resources. However, the towers located at these places are often struck by lightning. For an optimal lightning protection design of a new wind power plant and a lightning-risk evaluation of the existing wind power plants, transient characteristics of the tower, i.e., a vertical conductor should be clarified [1]. An electromagnetic field analysis is suitable for this investigation since the tower characteristics are hardly obtained by experiments. The method becomes practical by improvements of computational abilities. They are, however, not sufficient for the lightning surge estimation of power systems such as wind farms. Although circuit analysis method is appropriate for the analysis, the vertical conductor has to be represented by a numerical model.

Various circuit models of the vertical conductor have been proposed based on the Neumann's formula [2]-[4], experimental results [5], [6], and numerical electromagnetic analysis results [7]-[9]. Some models [6], [8] take into account the frequency-dependent effect of a vertical conductor by applying the Semlyen's line model installed in Electromagnetic Transients Program (EMTP).

This paper presents a modeling method of a vertical conductor, which considers frequency-dependent effects and direction-dependent characteristics of traveling waves, using results by Finite-Difference Time-Domain (FDTD) method. The model is expressed by MODELS, which is built in EMTP. An experiment using a reduced-size wind tower model is carried out to confirm the reliability of the proposed model.

A. Yamanaka, A. Hori, H. Murakami, and N. Nagaoka are with the Department of Electrical Engineering, Doshisha University, Kyoto, Japan (e-mail of corresponding author: oyasasi.bfg25@gmail.com).

Paper submitted to the International Conference on Power Systems Transients (IPST2017) in Seoul, Republic of Korea June 26-29, 2017

II. FDTD Simulation

Virtual Surge Test Lab (VSTL), which is developed by Central Research Institute of Electric Power Industry (CRIEPI), is used for the FDTD calculations [10].

The FDTD calculations are carried out in the following two cases: (A) a current wave expressed by (1) is injected into the bottom of a vertical conductor, and (B) the current is injected into the top of the vertical conductor. In Cases (A) and (B), the vertical conductor is set afloat above a perfectly conducting ground.

$$i_{in}(t) = I_{in}\left\{1-\exp\left(-\frac{t}{\tau_i}\right)\right\} \tag{1}$$

I_{in} and τ_i are set to 1 A and 1 ns, respectively.

The simulation spaces are illustrated in Fig. 1. The current is injected at the center of the conductor by a current source whose internal impedance is infinity. The FDTD analysis space is 8.125 × 8.125 × 6.175 m (= $x \times y \times z$) and is divided into cubic cells whose side length is 32.5 mm. The second order Liao's absorbing boundary condition is applied to the boundary. A calculation time step Δt is set to 62.5 ps based on the Courant condition.

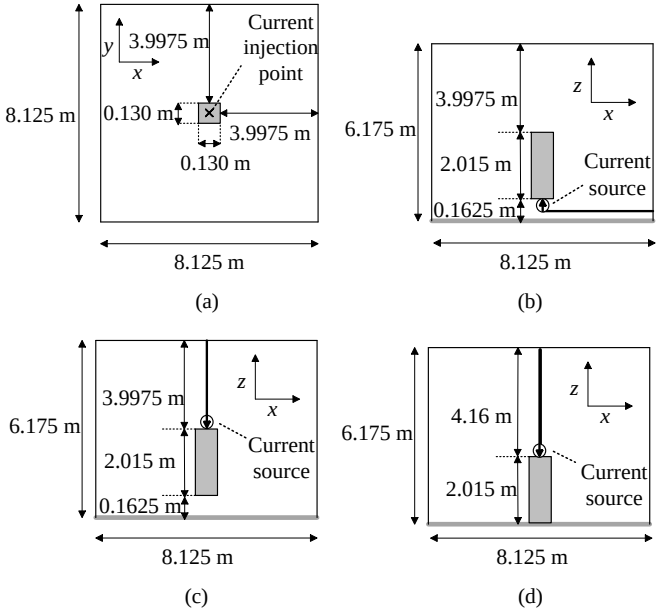

Fig. 1. Configuration of the FDTD analysis. (a) illustrates the *x*-*y* plane of the analysis space of all cases, (b) illustrates the *x*-*z* plane of Case (A): the current is injected into the bottom of the floated vertical conductor, (c) is for Case (B): the current is injected into the top of the floated vertical conductor, and (d) is Case (C): the current is injected into the top of the grounded vertical conductor.

The vertical conductor is a 1/40 reduced-size model of a 2.5 MW class wind turbine tower. It is expressed by a square perfect conductor, whose length and side length are 2.015 m (62 cells) and 130 mm (4 cells), respectively. The circumference of the tower model is equal to that of the pipe, which is used for an experiment in Section IV-A. The conductor is arranged above 162.5 mm (5 cells) from the earth surface.

A conductor voltage is defined as an integration of the electric field from the absorbing boundary to the conductor. The injected, sending-end, and receiving-end currents are derived as an integration of the magnetic field around the conductor.

An additional case is appended for a reliability test of the circuit model: (C) the current is injected into the top of a vertical conductor that is directly grounded to the perfectly conducting ground.

III. Circuit Model of a Vertical Conductor

A. Derivation of Model Parameters

The current and voltage waveforms calculated by means of FDTD method should be transformed from a time domain into a frequency domain in order to obtain model parameters expressing the vertical conductor. In a numerical Fourier or Laplace transform, the truncation and aliasing errors are unavoidable. In this paper, the current and the voltage waveforms are transformed into frequency domain using analytical Laplace transform to avoid the numerical errors. For the analytical calculation, the voltage waveforms are approximated by exponential functions expressed in (2) and are transformed into *s*-domain [11].

$$v_{apr}(t) = u(t-t_d)\left[\begin{array}{l} V_0\left\{1-\exp\left(-(t-t_d)/\tau_i\right)\right\}+ \\ \sum_{k=1}^{N} V_k\left\{\begin{array}{l}\exp\left(-(t-t_d)/\tau_i\right) \\ -\exp\left(-(t-t_d)/\tau_k\right)\end{array}\right\}\end{array}\right] \qquad (2)$$

$$V_{apr}(s) = \mathcal{L}\left\{v_{apr}(t)\right\} = \frac{\exp(-st_d)}{1+s\tau_i}\left(\frac{V_0}{s}+\sum_{k=1}^{N} V_k\frac{\tau_k-\tau_i}{1+s\tau_k}\right)$$

where $\mathcal{L}$ and s denote Laplace transform and its operator.

The voltage waveforms are approximated until the arrival of the reflection waves. The delay time t_d expresses the propagation time of the traveling wave and is defined by the length and a light velocity for the receiving-end voltage. The delay t_d is zero for the sending-end voltage. The parameters V_0, V_k, and τ_k are determined by a nonlinear least squares method based on sequential quadratic programing method.

The approximated voltage shown in (2) contains the time constant τ_i of the current in order to make the impedance independent of the injected current waveform. Calculated waveforms by FDTD method and the results of their approximations are shown in Fig. 2.

The sending-end current waveform has to be approximated by the function shown in (1) because some of the injected current leaks via a stray capacitor, i.e., all of the current cannot be injected into the vertical conductor. The sending-end current is also approximated until the arrival of the reflection wave. Even if the receiving-end is open-circuited, the current at the node leaks via a stray capacitor. The injected, sending-end and receiving-end currents are shown in Fig. 3.

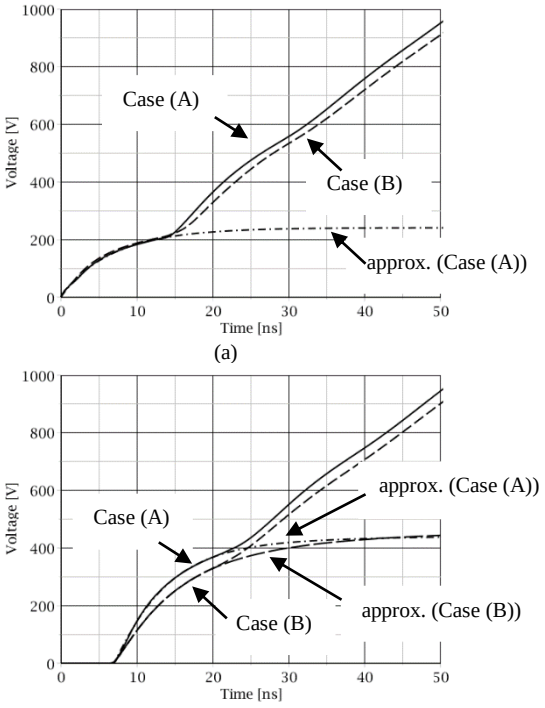

Fig. 2. Voltage waveforms calculated by FDTD method and their approximations in Cases (A) and (B). (a) shows waveforms at the sending-end, and (b) shows those at the receiving-end.

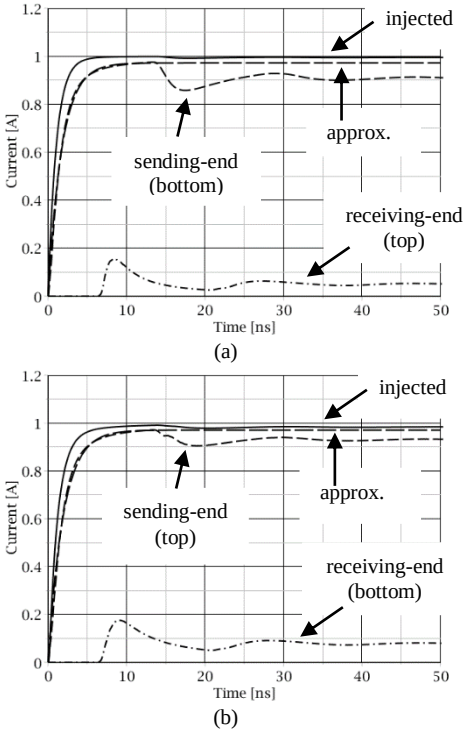

Fig. 3. An injected, sending-end currents with their approximations, and receiving-end currents calculated by FDTD method. (a) shows case (A): a current is injected into the bottom, and (b) shows case (B): a current is injected into the top. An approximated sending-end current is expressed by a long-broken line.

The characteristic impedance is given in a frequency domain as a ratio between the approximated sending-end voltage and the current.

$$Z_0(s) = V_s(s) / I_s(s) \tag{3}$$

The propagation characteristic for the traveling wave propagating each direction is defined as a ratio between the sending-end voltage $V_s(s)$ and the traveling wave at the receiving-end $V_r(s)/(1+\theta_r)$.

$$\exp(-\Gamma l) = \frac{V_r(s)}{(1+\theta_r)} \frac{1}{V_s(s)}, \qquad \theta_r = (Z_r - Z_0)/(Z_r + Z_0) \tag{4}$$

where Γ is the propagation constant, l is the conductor length, θ_r is the reflection coefficient, and Z_r is the impedance connected to the vertical conductor at the receiving end.

Though the vertical conductor illustrated in Fig. 1 is open circuited in the FDTD calculation, a stray capacitor C_s has to be considered as Z_r in (4) to express the leakage current at each node. The stray capacitor C_s is calculated from the slope of the integrated current waveform vs. the voltage at the receiving-end. The stray capacitances of 2.5 pF and 4.0 pF are derived from the Cases (A) and (B), respectively.

A phase rotation n in (5) has to be taken account in the calculation of the propagation constant Γ. The rotation n is counted considering its physical meaning.

$$\Gamma = -\ln\left(\exp(-\Gamma l)\right)/l = -\ln\left(|\exp(-\Gamma l)|\, e^{j\theta}\right)/l = -\left\{\ln\left(|\exp(-\Gamma l)|\right) + j(\theta + 2n\pi)\right\}/l \tag{5}$$

B. Line Parameters

In a homogenous distributed parameter theory, a line series impedance and a parallel admittance for per unit length are defined. On the other hand, such parameters cannot be defined for a vertical conductor because they depend on their position, i.e., height. Although there is a little influence of the ground on a downward traveling wave, the effect is large on the propagation characteristics of an upward traveling wave. The characteristic impedances and propagation constants of the upward traveling wave are different from those in the downward traveling wave.

Fig. 4 shows the amplitudes of the characteristic impedances in a frequency domain calculated by (3). In a high frequency region, the characteristic impedance at the bottom of the vertical conductor is smaller than that at the top. This can be explained that the characteristic impedance converges to the square root of L/C with an increase of frequency, and the line parallel capacitance C at the bottom of the vertical conductor is larger than that at the top.

Fig. 5 shows the attenuations of the up- and down-ward traveling waves. The downward traveling wave significantly attenuates compared with the upward travelling wave. Fig. 6 shows the propagation velocities of the traveling waves. The downward traveling wave propagates slower than the upward traveling wave.

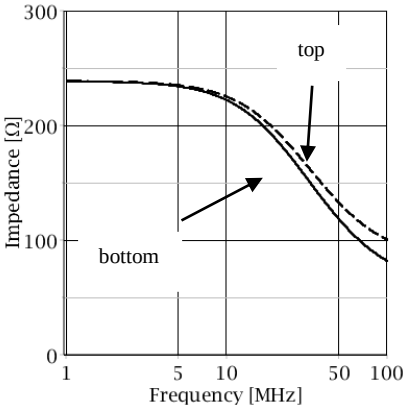

Fig. 4. Amplitude of the characteristic impedances in a frequency domain. The solid line (bottom) and dash line (top) express the characteristic impedance calculated from Cases (A) and Case (B), respectively.

The line parallel capacitance increases gradually for the downward traveling wave as it propagates from the top to the bottom of the vertical conductor. Because of this feature, the apparent line parallel capacitance for the downward traveling wave is larger than that for the upward traveling wave. The difference in the apparent line capacitance causes the difference in the attenuation and the propagation velocity of the traveling waves.

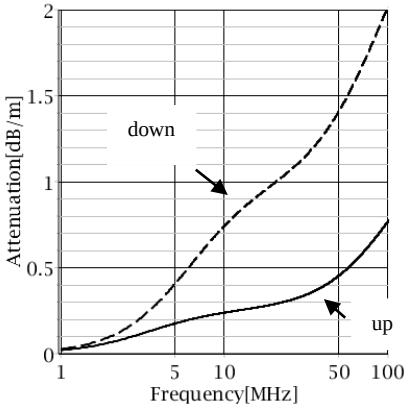

Fig. 5. Wave attenuations of the traveling waves propagating along a vertical conductor in a frequency domain. The solid line (up) denotes the attenuation of the upward traveling wave derived from Case (A). The dash line (down) is for Case (B).

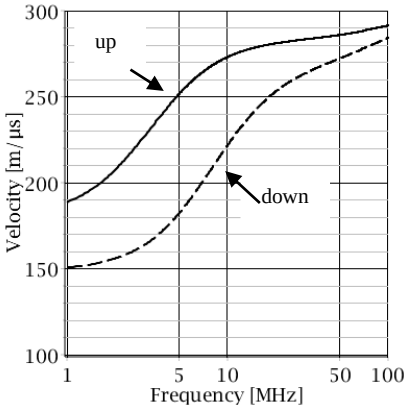

Fig. 6. Propagation velocities of the traveling waves. The solid line (down) and dash line (up) show the velocity of the downward traveling wave calculated from Cases (B) and (A), respectively.

C. Equivalent Circuit of a Vertical Conductor

Fig. 7 illustrates a schematic diagram of the traveling waves propagating along a single phase distributed parameter line, which has the different characteristic impedances and the propagation constants.

The terminal voltages V_t and V_b, and the currents I_t and I_b are given in (6) using the traveling waves V_{td} and V_{bu}.

$$\begin{aligned} V_t &= V_{td} + \exp\left(-\Gamma_u l\right) V_{bu} \\ I_t &= \left\{V_{td} - \exp\left(-\Gamma_u l\right) V_{bu}\right\} / Z_{0d} \\ V_b &= \exp\left(-\Gamma_d l\right) V_{td} + V_{bu} \\ I_b &= -\left\{\exp\left(-\Gamma_d l\right) V_{td} - V_{bu}\right\} / Z_{0u} \end{aligned} \tag{6}$$

where Z_{0d} and Z_{0u} denote the characteristic impedances at the top and the bottom of the conductor, respectively. The propagation constants Γ_u and Γ_d express the parameters for the upward and downward traveling waves.

The injected currents into the terminals in (7) are obtained from (6) by eliminating the traveling waves.

$$\begin{aligned} I_t &= \frac{V_t}{Z_{0d}} - \exp\left(-\Gamma_u l\right)\left(\frac{V_b}{Z_{0d}} + \frac{Z_{0u}}{Z_{0d}} I_b\right) = \frac{V_t}{Z_{0d}} + J_d \\ I_b &= \frac{V_b}{Z_{0u}} - \exp\left(-\Gamma_d l\right)\left(\frac{V_t}{Z_{0u}} + \frac{Z_{0d}}{Z_{0u}} I_t\right) = \frac{V_b}{Z_{0u}} + J_u \end{aligned} \tag{7}$$

An equivalent circuit of a vertical conductor is obtained from (7). The circuit illustrated in Fig. 8 is expressed by the characteristic impedances Z_{0d} and Z_{0u}, and current sources J_d and J_u. The circuit is suitable for a circuit simulation based on nodal analysis method. Each current source stores the past history of the voltage and current at the other node. The circuit model is installed in EMTP using MODELS type-94 nonlinear element. The characteristic impedances Z_{0d} and Z_{0u}, and the propagation characteristics $\exp(-\Gamma_u l)$ and $\exp(-\Gamma_d l)$ are expressed by rational functions in s-domain [12], [13].

Case (C) for the FDTD analysis explained in Chapter II is simulated by EMTP. The stray capacitance of 2.5 pF explained in Section III-A is inserted at the top of the vertical conductor model in order to express the leakage current.

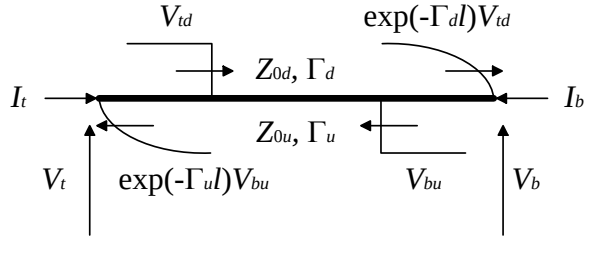

Fig. 7. A single phase distributed parameter line which has different characteristic impedances and propagation constants depending on the direction of the traveling wave.

Some EMTP simulations are carried out in the following four cases. In Case (i), a constant characteristic impedance model given by a solution of Neumann's formula [6] is used (const.). In Cases (ii) and (iii), the characteristic impedances and propagation characteristics are assumed to be those of the upward model and downward model, respectively (up, and down). Case (iv) is for the proposed model, which takes into account both up- and down-ward characteristics (proposed).

Fig. 9 shows the simulation results of the above cases with the result of FDTD method, which accurately takes into account the propagation characteristic of the vertical conductor. As shown in Fig. 9 (a), the constant parameter model (Case (i)) cannot express the FDTD simulation result. The frequency-dependent characteristics should be considered for the surge analysis of the vertical conductor.

From Fig. 9 (b) and (c), it is clear that there are differences in the attenuation and oscillating frequency if the unilateral characteristics are used. Fig. 9 (d) shows that the proposed model accurately reproduces the FDTD calculation result. The direction-dependent characteristics have a large influence and should be taken into consideration for a transient simulation of the vertical conductor.

IV. Experiment Using Reduced-Size Model

A. Experimental Conditions

Fig. 10 illustrates an experimental setup using a reduced-size wind turbine tower model. The tower is modeled by an aluminum pipe, whose height, radius, and thickness are 2.0 m, 82.5 mm, and 2.5 mm, respectively. The pipe is arranged 65 mm above a 4×11 m aluminum plate. A current is injected into the bottom of the pipe via a coaxial cable with a resistor of 1 kΩ, R_s.

The conductor voltage at the top is defined as the potential difference between the top of the conductor and a voltage reference wire, which is grounded to the aluminum plate. The voltage at the bottom is defined as the potential difference between the bottom of the conductor and the aluminum plate just below the conductor. Each voltage is measured by a voltage probe P5100A and the injected current is measured by a current probe CT-1 (Tektronix), respectively. Because of the difference in the length of the probes, the conductor voltage and the injected current are separately measured. The pulse generator (P.G.) generates a pulse wave by releasing charges stored inside the cable.

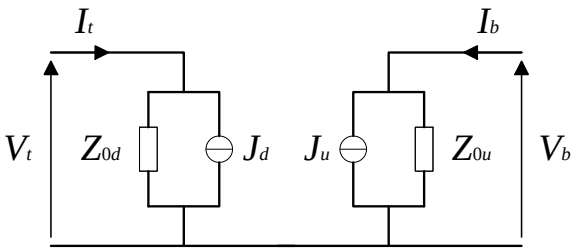

Fig. 8. An equivalent circuit of a vertical conductor which has different characteristic impedances and propagation constants depending on the direction of the traveling wave.

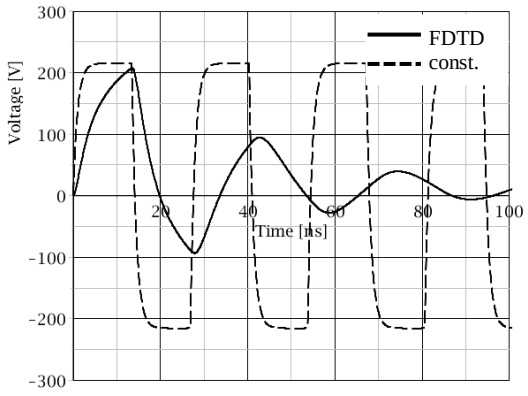

(a)

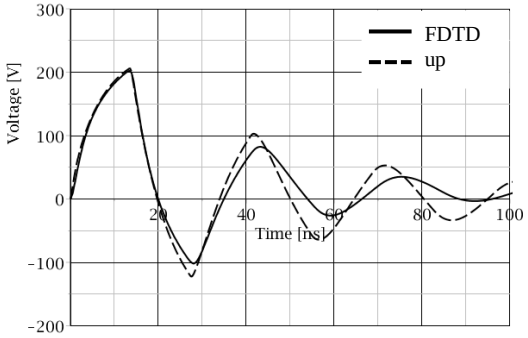

(b)

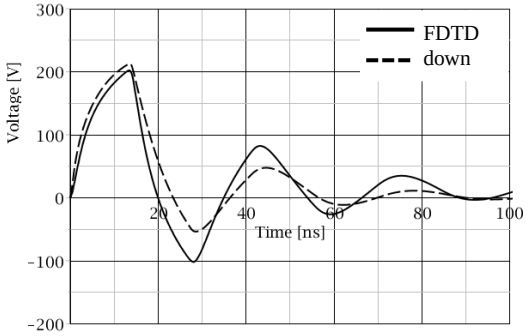

(c)

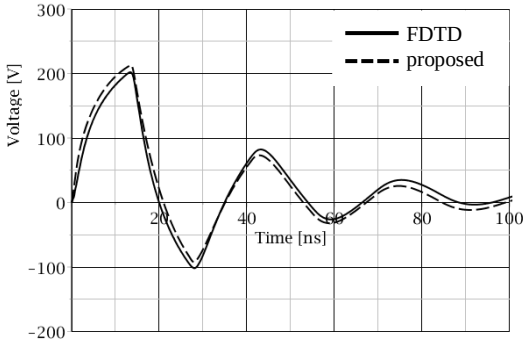

(d)

Fig. 9. Simulated results by FDTD method and EMTP for Case (C): current is injected into the top of the grounded vertical conductor. (a), (b), (c) and (d) show EMTP simulations for Cases (i), (ii), (iii), and (iv), respectively.

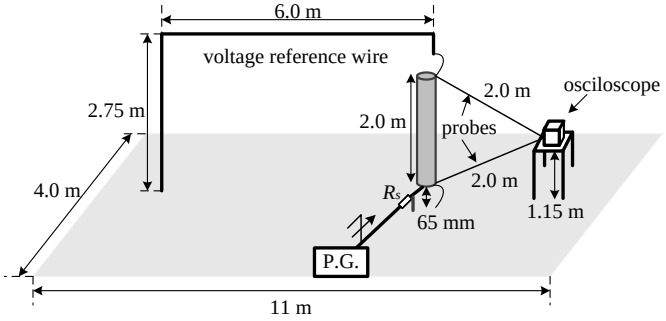

Fig. 10. An experimental setup using a reduced-size wind-turbine tower model.

B. Comparison of Measured and EMTP Results

Fig. 11 illustrates the circuit for simulating the experiment by EMTP. The line parameters of the coaxial cables RG55U (for P.G. model) and 3D2V (for current injection) are derived by Semlyen Setup, and are expressed by Semlyen's line model. The voltage probe is modeled by an *RC* parallel circuit (R_p = 40 MΩ and C_p = 2.5 pF) expressing its input impedance. For the current waveform simulation, voltage probe models are excluded as in the experiment.

The measured and EMTP simulated results are shown in Fig. 12. It is clear from the simulation results that the accuracy of the constant parameter model is low due to the ignorance of the frequency-dependent effect.

The accuracy of the proposed model which takes into account the upward and downward characteristics is higher than that of the other models. The up- and down-ward characteristics have to be independently included into the circuit model of the vertical conductor. The differences in the injected current, sending-end voltage, and the receiving-end voltage are smaller by 5 %. In addition to the frequency-dependent effect, the direction-dependent characteristics of the traveling wave are represented by the proposed model.

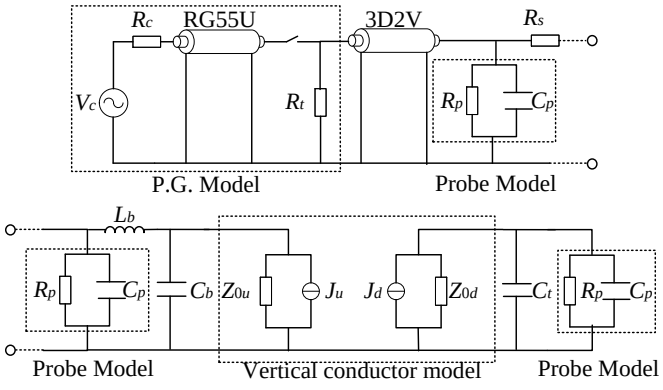

Fig. 11. EMTP simulation circuits for the experiment using a reduced wind turbine model. The upper figure is a current source, and the lower one is the vertical conductor model with probe models. The vertical conductor is expressed by MODELS type-94 nonlinear element.

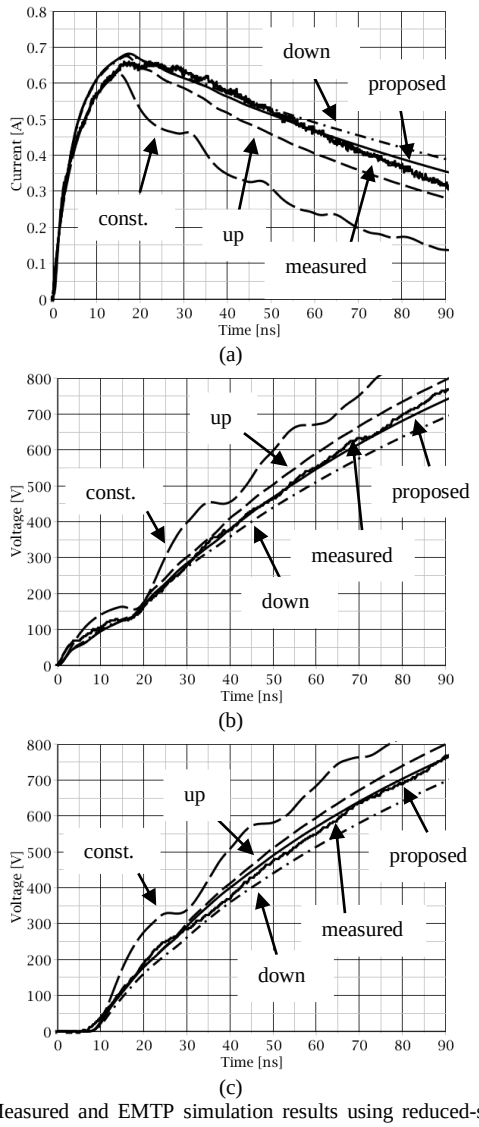

Fig. 12. Measured and EMTP simulation results using reduced-size tower model. (a) shows the injected current waveforms, (b) shows the sending-end voltage waveforms, and (c) shows the receiving-end voltage waveforms.

V. Conclusions

A method synthesizing a distributed parameter line model of a vertical conductor is proposed in this paper. The model parameters are obtained from the calculated results by FDTD method. The frequency-dependent effect and direction-dependent characteristics of the vertical conductor are expressed in a circuit analysis by using MODELS, which is built in EMTP. The accuracy of the proposed model is confirmed by comparisons between the simulation results of EMTP and the measurement results from a reduced-size tower model.

The transient responses of the vertical conductor, which is set afloat above a perfect conducting ground, are calculated by means of FDTD method. A current is injected into the top or the bottom of the vertical conductor in order to separately derive the characteristics for up- and down-ward traveling waves. The voltage and the current waveforms are approximated by some exponential functions using a nonlinear least squares method. The approximated waveforms are analytically transformed into a frequency domain without truncation and aliasing errors. Because the characteristic impedances and the propagation characteristics are expressed by rational functions in *s*-domain, they are easily installed in EMTP.

The proposed model introduces the advantages of the electromagnetic field analysis, which automatically considers the characteristics of the vertical conductor, to the circuit analysis tools. The proposed method is applicable for a wind turbine tower built on earth surface.

VI. Acknowledgment

The authors are very grateful to Prof. Yoshihiro Baba at Doshisha University for his advice and guidance.

VII. References

[1] New Energy and Industrial Technology Development Organization (NEDO), “Countermeasure to lightning” in: Guideline of Wind Power Generation for Japan, 2008.

[2] A. Ametani, Y. Kasai, J. Sawada, A. Mochizuki, and T. Yamada, “Frequency-dependent impedance of vertical conductors and multi conductor tower model” *Proc. Inst. Elec. Eng. Gener. Transmiss. Distrib*., vol.141, no.4, pp.339-345, 1994.

[3] A. De Conti, S. Visacro, A. Soares, Jr., and M.A.O. Schroeder, “Revision, extension, and validation of Jordan’s formula to calculate the surge impedance of vertical conductors”, *IEEE Trans. EMC*, vol.48, no.3, pp.530-536, 2006.

[4] P. Gomez, “Definition of a new formula for the characteristic impedance of vertical conductors for lighting transients”, *Proc. Int. Conf. on Power Systems Transients (IPST) 2013*, Cavtat, Croatia, June 15-18, 2013.

[5] T. Hara, O. Osamu, M. Hayasi, and C. Uenosono, “Empirical Formulas of Surge Impedance for Single and Multiple Vertical Cylinder”, *Trans. IEEJ*, vol.110-B, no.2, pp.129-137, 1990.

[6] N. Nagaoka, “A Development of Frequency-Dependent Tower Model”, *Trans of IEEJ*, vol.111-B, no.1, pp.51-56, 1991.

[7] T. Noda, “A Tower Model for Lightning Overvoltage Studies Based on the Result of an FDTD Simulation”, *IEEJ Trans. PE*, vol.127, no. 2, pp.379-388, 2007.

[8] Y. Ikeda, N. Nagaoka, Y. Baba, and A. Ametani, “A frequency dependent circuit model of a wind turbine tower using transient response calculated by FDTD”, *The Paper of International Conference of Lightning Protection (ICLP)*, Vienna, Austria, 2012.

[9] Y. Ikeda, N. Nagaoka, and Y. Baba, “A Circuit Model for Lightning Surge of Wind Turbine Tower with an Internal Conductor”, *IEEJ Trans. PE*, vol.135, no.3, pp.200-206, 2015.

[10] T. Noda and S. Yokoyama, “Development of a General Surge Analysis Program Based on the FDTD method”, *Trans. of IEEJ*, vol.121-B, no.5, pp.625-632, 2001.

[11] A. Hori, H. Tanaka and N. Nagaoka, “Rail Model for Lightning Surge Analysis Based on FDTD Simulation Results”, *IWHV&JK*, 2016.

[12] Canadian / American EMTP User Group, “ATP Rule Book”, 1999.

[13] T. Noda and L. Dube, “Simulation Model Description Language MODELS”, Japanese EMTP Committee, 1996.